DIRECT POWER CONTROL OF GRID CONNECTED PHOTOVOLTAIC SYSTEM WITH LINEAR REORIENTED COORDINATE METHOD AS MAXIMUM POWER POINT TRACKING ALGORITHM

SALIM BOUCHAKOUR[1], AHMED TAHOUR[2], HOUARI SAYAH[3],
KAMEL ABDELADIM[1,4] AISSAOUI ABDELGHANI[4]

Keywords: Grid connected photovoltaic system, Direct power control, Linear reoriented coordinate method, Modeling, Simulation.

In this study, we present a control algorithm for grid connected photovoltaic (PV) system on two stage converters, where a DC-DC converter is connected between the PV array and the DC-AC converter. The DC-DC converter performs the maximum power point tracking (MPPT) and the voltage amplification. The linear reoriented roordinates (LRC) method is used as a boost converter controller in order to allow the PV array to operate at maximum power for any weather conditions. The DC-AC converter transfers the maximum power extracted from the PV array into the grid. The direct power control (DPC) has been used to control the pulse width modulation (PWM) inverter. The modeling and the control are carried out using MATLAB/ Simulink environment. The simulation results are presented with the validation of grid connected PV system performance and the chosen control schemes.

1. **INTRODUCTION**

Nowadays an increasing part of electrical energy is generated using renewable energy sources (RES), where the power electronic converters are present. There are two kinds of RES which are the most prevalent, wind and solar energy. However, our country holds one of the most important solar potential which gives the advantage to the photovoltaic (PV) system installation compared to wind energy, which can be used almost in every place with an appropriate setting up of PV arrays. Isolated systems were pioneers, because it was the more adequate and practical (less costs and weight) to provide the amount of energy necessary for long periods of staying in space during the space race. The same ones were largely used as energy sources for systems installed in remote areas. Systems connected directly to the network arose in the beginning of 90's and rapidly spread out in developed

[1] Centre de Développment des Energies Renouvelables, Bouzaréah, Algiers 16000, Algeria
[2] University of Mascara, 29000 Algeria. tah_ahmed13@yahoo.fr
[3] Département d'électrotechnique, Université de Sidi Bel Abbes, 22000 Algeria
[4] Laboratoire IRECOM, Université de Sidi Bel Abbes, 22000 Algeria

countries, strengthened mostly by solids investments of the governments. The main advantage of this configuration is that, besides reducing costs due to the fact that accumulators are not required, it generates extra energy compared to the charge's consumption, and this excess can be injected straight to the grid. When the system generates less than it is required to support the demand, the energy is then extracted from the grid [1]. The PV system integration to the power system can be done in one stage with the application of a voltage source inverter or in two stages with the application of both DC-DC converter and inverter [2]. This paper presents a three-phase topology, composed of a DC-DC converter cascaded to a PWM inverter.

In order to improve the performance of the PV system, the LRC method has been proposed to control the DC-DC converter and transfer the maximum power from PV array to the inverter. For inverter's control, the direct power control (DPC) method has been selected to be presented throughout this paper. The effectiveness of the proposed control schemes has been established via MATLAB/Simulink.

2. **MODEL DESCRIPTION OF THE GRID CONNECTED PV SYSTEM**

Figure 1 shows the electric power system and control schemes proposed to interface the photovoltaic array with the power grid. The first stage is the boost converter, which will raise the relatively low solar voltage to a suitable level (550 V) and perform the maximum power point tracking (MPPT) for the DC link bus. The second stage is the DC to AC converter that the switching states are selected by a switching table based on the errors between the commanded and estimated values of active and reactive power.

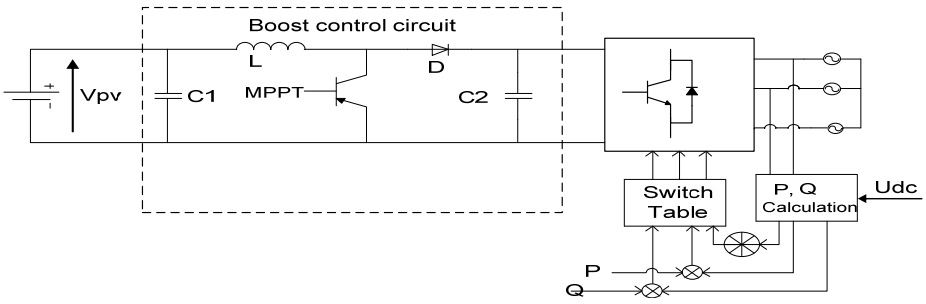

Fig. 1 – Block diagram of proposed electric power and control schemes.

3. **PHOTOVOLTAIC MODULE MODELING**

The PV module is the unity of base for the construction of a PV array. We have used the PV module model proposed by Eduardo [3, 4]. The current-voltage relationship is given by:

$$I(V) = \frac{I_{sc\_x}}{1 - e^{\frac{-1}{b}}} \left[1 - e^{\left(\frac{V}{bV_{oc\_x}} - \frac{1}{b} \right)} \right] \tag{1}$$

The model includes a short circuit current I_{sc_x} and open circuit voltage V_{oc_x} can be obtained using equations:

$$V_{sc\_x} = s\frac{E_i}{E_{in}} TCv(T_{cell} - T_n) + sV_{oc\_\max} - sV_{oc\_\max} e^{(\frac{E_i}{E_{in}})} (\frac{V_{oc\_\max} - V_{oc\_ref}}{V_{oc\_\max}}), \tag{2}$$

$$I_{sc\_x} = p\frac{E_i}{E_{in}} \left[I_{scref} + TCi(T_{cell} - T_n) \right]. \tag{3}$$

I_{sc_ref} and V_{oc_ref} are the short circuit current and open circuit voltage. V_{oc_max} is the open-circuit voltage. T_{cell} is the solar cell temperature in °C with T_n = 25°C. E_i is the effective solar irradiation in W/m² with E_{in} = 1 000 W/m². T_{Cv} is the temperature coefficient of V_{oc} in V/°C. T_{Ci} is the temperature coefficient of I_{sc} in A/°C. The variable *s* is the number of PV panels with the characteristics connected in series and *p* is the number of PV panels with characteristics connected in parallel.

4. **BOOST CONVERTER MODELING**

Figure 1 shows the equivalent circuit of the boost converter. These converters can be described using ordinary differentiation equations as follows:

$$I_{Lboost} = I_{pv} - C_1 \frac{dU_{pv}}{dt}, \tag{4}$$

$$I_{dc} = (1 - D) I_{Lboost} - C_2 \frac{dU_{dc}}{dt}, \tag{5}$$

$$V_{pv} = (1 - D) V_{dc} - L \frac{dI_{Lboost}}{dt}. \tag{6}$$

D is the duty cycle, the switch is "on" for a period equal to *DT*, and the switch is "off" for an interval time equal to (1 – *D*) *T*.

I_{pv} and V_{pv} are the output current and the output voltage of PV array. C_1, L_{boost}, *D*, C_2 are the input capacitor, the inductor, diode and output capacitor respectively.I_{dc} and U_{dc} are the output current and the output voltage of boost converter.

4.1 MAXIMUM POWER POINT TRACKING

The maximum power point tracking (MPPT) algorithms has different versions of numerical iterations, long and tedious, that relate the derivative of the current with respect to the voltage equaled to the negative of the current divided by the voltage. Unlike the use of LRC method as MPPT algorithm can be a very powerful and a simple way to approximate the maximum power point (MPP). LRC method uses to obtain a close approximation of the *I-V* curve knee point. The *I-V* curve knee point is the optimal current I_{mpp} and voltage V_{mpp} that produces P_{max}, (Fig.2).

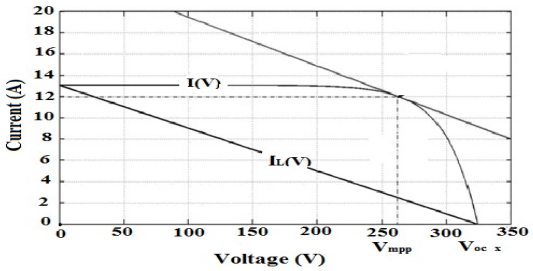

Fig. 2 – *I-V* curve and LRC methode.

A linear current quation $I_L(V)$ can be given in (7).

$$I_L(V) = I_{sc\_x} - I_{sc\_x}\frac{V}{V_{oc\_x}}. \tag{7}$$

The derivatives of $I(V)$ and $I_L(V)$ are given by (8) and (9).

$$\frac{\partial I_L(V)}{\partial V} = \frac{-I_{sc\_x}}{V_{oc\_x}}, \tag{8}$$

$$\frac{\partial I}{\partial V} = \frac{-I_{sc\_x}\,\mathrm{e}^{\left(\frac{V}{bV_{oc\_x}}-\frac{1}{b}\right)}}{bV_{oc\_x} - bV_{oc\_x}\,\mathrm{e}^{\frac{-1}{b}}}. \tag{9}$$

In LRC method, the slope of the *I-V* curve at the knee point is approximated by equation (10) The approximate optimal voltage V_{mpp} is given by (11):

$$\frac{\partial I_L(V)}{\partial V} \approx \frac{\partial I(V)}{\partial V} \Rightarrow \frac{-I_{sc\_x}}{V_{oc\_x}} \approx \frac{-I_{sc\_x}\,\mathrm{e}^{\left(\frac{V}{bV_X}-\frac{1}{b}\right)}}{bV_{oc\_x} - bV_{oc\_x}\,\mathrm{e}^{\frac{-1}{b}}}, \tag{10}$$

$$V_{mpp} = V_{oc\_x} + b.V_{oc\_x} \ln(b - be^{\frac{-1}{b}}) . \quad (11)$$

We can substitute V_{mpp} into (1) to obtain I_{mpp}, then to approximate P_{max}.

$$I_{mpp} = I_{sc\_x} \frac{1 - b + b\,e^{\frac{-1}{b}}}{1 - e^{\frac{-1}{b}}}, \quad (12)$$

$$P_{\max} = V_{mpp} I_{mpp} . \quad (13)$$

4.2. OPTIMAL DUTY CYCLE

Table 1 shows the conditions and the optimal duty cycle for buck converter, boost converter and buck-boost converter for load matching, where: R_{load} – load resistance and R_{op} – optimal resistance.

Table 1

Converter	Optimal duty cycle	Conditions
Buck - Boost	$D = \frac{V_{dc}}{V_{dc} + V_{mpp}}$	none
Boost	$D = 1 - \frac{V_{mpp}}{V_{dc}}$	$R_{load} > R_{op}$
Buck	$D = \frac{V_{mpp}}{V_{dc}}$	$R_{load} < R_{op}$

5. **DIRECT POWER CONTROL OF PWM INVERTER**

Figure 3 shows the configuration of the direct instantaneous active and reactive power controller for the PWM inverter.

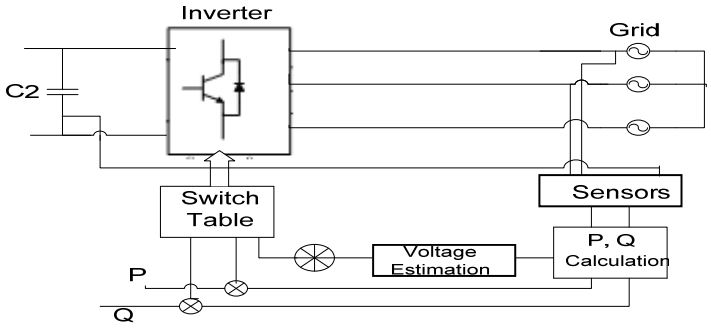

Fig. 3 – Grid connected PWM inverter circuit and the direct power control configuration.

The commands of reactive power q_{ref} and active power p_{ref} are compared with the estimated reactive (q_{est}) and active (p_{est}) values, in reactive and active power hysteresis controllers. The output signal of the reactive power controller is defined:

$$\begin{cases} S_q = 1 & \text{for} \quad p < p_{ref} - H_q \\ S_q = 0 & \text{for} \quad p > p_{ref} - H_q \end{cases}, \tag{14}$$

and similarly of the active power controller as:

$$\begin{cases} S_p = 1 & \text{for} \quad p < p_{ref} + H_p \\ S_p = 0 & \text{for} \quad p > p_{ref} + H_p \end{cases}, \tag{15}$$

where: H_q and H_p are the hysteresis bands.

The region of the voltage or flux vector position is divided into twelve sectors, as shown in Fig. 4.

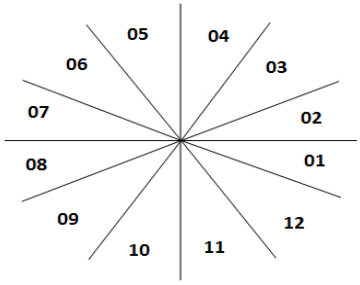

Fig. 4 – Sector selection for DPC

5.1. INSTANTANEOUS POWER ESTIMATION

The instantaneous values of active (p_{est}) and reactive power (q_{est}) in AC voltage sensorless system are estimated by:

$$p_{est} = L\left(\frac{\mathrm{d}i_a}{\mathrm{d}t} i_a + \frac{\mathrm{d}i_b}{\mathrm{d}t} i_b + \frac{\mathrm{d}i_c}{\mathrm{d}t} i_c\right) + U_{dc}\left(S_a i_a + S_b i_b + S_c i_c\right), \tag{16}$$

$$q_{est} = \frac{1}{\sqrt{3}}\left[3L\left(\frac{\mathrm{d}i_a}{\mathrm{d}t} i_c - \frac{\mathrm{d}i_c}{\mathrm{d}t} i_a\right) - U_{dc}\left[\left(S_a(i_b - i_c) + S_b(i_c - i_a) + S_c(i_a - i_b)\right)\right]\right]. \tag{17}$$

5.2. DYNAMIC PERFORMANCE

The combinations of each converter voltage space vector used for instantaneous active and reactive power variation are summarized in Table 2. Situation is presented for vector located in the *k* sector of α, β plane as shown in Fig. 5 [5].

Table 2

Instantaneous active and reactive variations due to the applied voltage vectors

	U_{k-2}	U_{k-1}	U_k	U_{k+1}	U_{k+2}	U_{k+3}	U_0U_7
q	- -	-	++	+	+	-	±
p	+	-	-	+	++	++	+

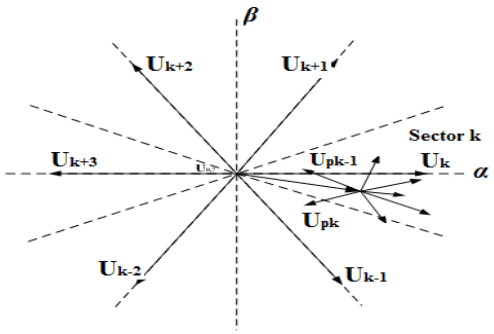

Fig. 5 – Variation of converter voltage space vector.

The digitized error signals and sector are input to the switching table in which every switching state, S_a , S_b and S_c, of the converter is stored, as shown in Table 3.

Table 3

Switching table

S_p	S_q	$Sect_1$	$Sect_2$	$Sect_3$	$Sect_4$	$Sect_5$	$Sect_6$	$Sect_7$	$Sect_8$	$Sect_9$	$Sect_{10}$	$Sect_{11}$	$Sect_{12}$
1	0	V_6 (101)	V_7 111)	V_1 (100)	V_0 (000)	V_2 (110)	V_7 (111)	V_3 (010)	V_0 (000)	V_4 (011)	V_7 (111)	V_5 (001)	V_0 (000)
	1	V_7 (111)	V_7 (111)	V_0 (000)	V_0 (000)	V_7 (111)	V_7 (111)	V_0 (000)	V_0 (000)	V_7 (111)	V_7 (111)	V_0 (000)	V_0 (000)
0	0	V_6 (101)	V_1 (100)	V_1 (100)	V_2 (110)	V_2 (110)	V_3 (010)	V_3 (010)	V_4 (011)	V_4 (011)	V_5 (001)	V_5 (001)	V_6 (101)
	1	V_1 (100)	V_2 (110)	V_2 (110)	V_3 (010)	V_3 (010)	V_4 (011)	V_4 (011)	V_5 (001)	V_5 (001)	V_6 (101)	V_6 (101)	V_1 (100)

6. **RESULT AND SIMULATION**

To study the operation of the proposed system under different solar irradiance conditions, the grid connected PV system and the whole control schemes have been simulated using the MATLAB/ Simulink software. For radiometric conditions, two cases of “sunny” and “cloudy” conditions have been considered for two typical days. The radiance and cell temperature profiles used are shown in Figs. 6 and 7.

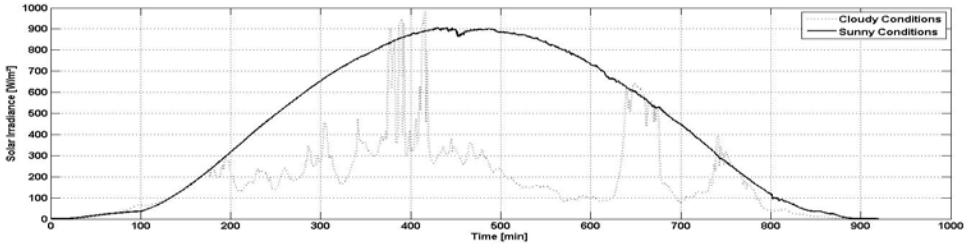

Fig. 6 – Irradiance profiles for sunny and cloudy conditions.

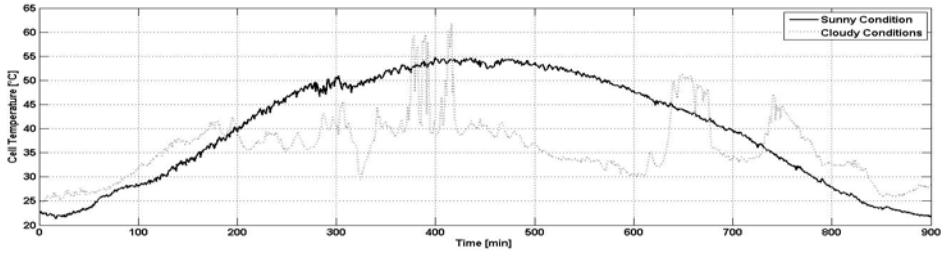

Fig. 7 – Cell temperature profiles for sunny and cloudy conditions.

Figure 8 shows the simulation results for PV array and DC-DC converter with LRC method as MPPT algorithm. These results show how effective is this method to calculate the optimal duty cycle and deliver the required power (P_{max}) using load matching for the two considered days.

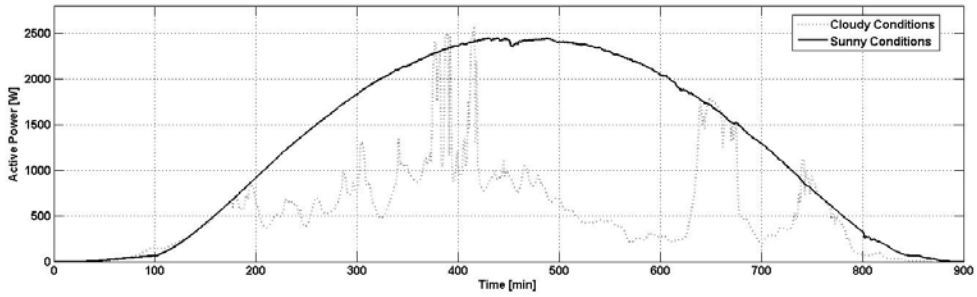

Fig. 8 – Active power produced by the PV array for sunny and cloudy conditions.

In Fig. 9, we can observe that the distribution network received the fluctuations from the active power[6]. The reactive power consumed by loads connected to the distribution network is mostly supplied by high voltage cables and capacitors installed on nearby buses of the medium voltage grid. Fast variations of reactive power supplied by photovoltaic systems, assuming very high densities of such systems, can cause fast capacitor switching [7]. The following results present the dynamic behavior of grid connected inverter controlled with DPC for the two considered days. These results were obtained for purely sinusoidal supply line voltage. As shown in Fig. 10, it can be seen that at any solar irradiance and temperature

conditions the inverter injects to the grid the maximum active power generated by PV array, under the unity power factor operation by setting the reactive power at zero [8].

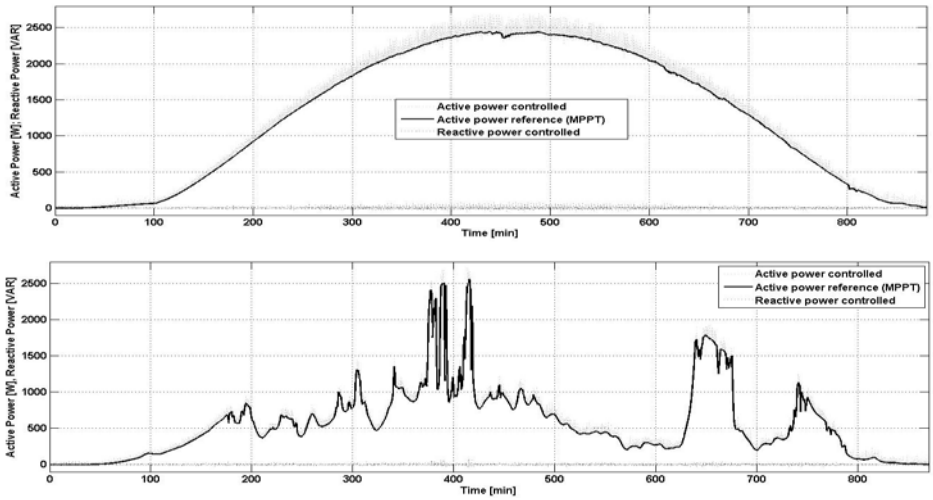

Fig. 9 – Active and reactive power injected to the grid: a) sunny conditions; b) cloudy conditions.

Figure 10, shows the simulated waveforms of the PWM inverter output voltage, the estimated grid voltage and the injected current to the grid for one phase. We observe the successfully estimation of the grid voltage and the sinusoidal waveform of the current injected. Also, the voltage and current grid are in phase, because the reactive power is set at zero [9].

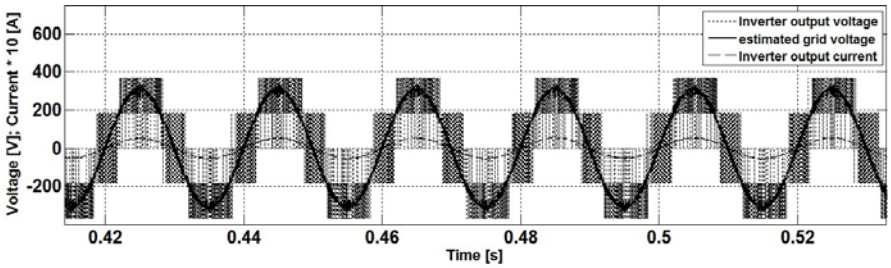

Fig. 10 – Output grid connected PWM inverter waveforms.

7. **CONCLUSION**

In this work we presented the modeling and the analysis of the three-phase grid connected photovoltaic generation system, including the PV array, DC-DC converter control and DC-AC converter control. A simple method called LRC was used as MPPT algorithm in order to provide the optimal duty cycle of the boost converter and active power reference for DPC of PWM inverter. The unity power

factor is achieved with the setting of the reactive power to zero. A dynamic behavior of the proposed control schemes are presented for two extreme scenarios (sunny and cloudy conditions).The simulation results confirmed that the proposed control combination gave us a good performance for regulation and injection of the maximum power to the grid at any weather conditions. Also, results showed a strong dependency between the THD and the generated power, in such a way that the THD is always high when the generated power is low.

APPENDIX

Electrical parameters of PV system power circuit:

PV array : nominal tension 12 V, max power, P_{max} 106 ±5%Wp (watts peak), I_{sc} = 6,54 A, open-circuit voltage,V_{oc}= 21,6 V, I_{max} = 6,1 A, V_{max} = 17,4 V, $_b$ = 0.098, T_{Cv} = 74 mV/°C, T_{Ci} = 2.3 mA/°C, number of modules in series, s 15; number of modules in parallels, p 2.

DC-DC converter (boost): output voltage 550 V, Smoothing capacitor C_1 = 20 µF, Boost Inductor L_{boost} = 200 mH.

DC-AC converter (Inverter): resistance reactors R , Inductance reactors L = 11.5 mH, Smoothing capacitor C_2 4700 µF, Power source voltage TRMS (true root mean square) V = 220 V.

Received on April 2, 2013

REFERENCES

1. K. C. A. de Souza, W. M. dos Santos, D. C. Martins, *Active and reactive power control in a single-phase grid-connected PV system with optimization of the ferrite core volume*, International Review of Electrical Engineering **6**, *7*, pp. 3142–3151, 2011.
2. G.T sengenes, G Adamidis, *A multi-function grid connected PV system with three level NPC inverter and voltage oriented control*, Solar Energy, **85**, *11*, 2011. pp. 2595–2610.
3. The Institute of Electrical and Electronics Engineers, *IEEE Recommended practice for utility Interface of photovoltaic (PV) systems*, IEEE Std. 929-2000, NY, April, 2000.
4. Ortiz-Rivera E., Peng F., *Analytical model for a photovoltaic module using the electrical characteristics provided by the manufacturer data sheet*, Power Electronics Specialists Conference, 2005. IEEE 36th, June 2005, pp. 2087–2091.
5. Sc. Mariusz Malinowski, *Sensorless Control Strategies forThree-Phase PWM Rectifiers*, Ph.D. Thesis, Institute of Control and Industrial Electronics, Faculty of Electrical Engineering, Warsaw University of Technology, 2001.
6. H. Muller, A. Rudolf, G. Aumayr, *Studies of Distributed Energy Supply Systems using an Innovative Energy Management System*, 22nd IEEE Power Engineering Society International Conference on Power Industry Computer Applications (Innovative Computing for Power-Electric Energy Meets the Market), May 2001, pp. 87–90.
7. M. Patsalides, D. Evagorou, G. Makrides, Z. Achillides, G. E. Georghiou, A. Stavrou, V. Efthimiou, B. Zinsser, W. Schmitt and J. H. Werner, *The Effect of Solar Irradiance on the Power Quality Behaviour of Grid Connected Photovoltaic Systems*, International Conference on Renewable Energy and Power Quality 2007 (ICREPQ 07), Sevilla, March 2007, pp. 1–7.
8. Srisaen N., Sangswang A., *Effects of PV Grid-Connected System Location on a Distribution System IEEE*, APCCAS, 2006, pp. 852-855.
9. Gianfranco Chicco, Jürgen Schlabbach, Filippo Spertino, *Experimental assessment of the waveform distortionin grid-connected photovoltaic installations*, Solar Energy, **83**, pp. 1026–1039, 2009.